HHS Public Access

Author manuscript

Cell Rep. Author manuscript; available in PMC 2016 August 18.

Published in final edited form as:

Cell Rep. 2015 August 18; 12(7): 1107–1119. doi:10.1016/j.celrep.2015.07.015.

Macrophages Contribute to the Spermatogonial Niche in the Adult Testis

Tony DeFalco[1,*], **Sarah J. Potter**[1], **Alyna V. Williams**[1], **Brittain Waller**[1], **Matthew J. Kan**[2], and **Blanche Capel**[3]

[1]Division of Reproductive Sciences, Cincinnati Children's Hospital Medical Center, Cincinnati, OH 45229 USA

[2]Department of Immunology, Duke University Medical Center, Durham, NC 27710 USA

[3]Department of Cell Biology, Duke University Medical Center, Durham, NC 27710 USA

Summary

The testis produces sperm throughout the male reproductive lifespan by balancing self-renewal and differentiation of spermatogonial stem cells (SSCs). Part of the SSC niche is thought to lie outside the seminiferous tubules of the testis; however, specific interstitial components of the niche that regulate spermatogonial divisions and differentiation remain undefined. We identified distinct populations of testicular macrophages, one of which lies on the surface of seminiferous tubules in close apposition to areas of tubules enriched for undifferentiated spermatogonia. These macrophages express spermatogonial proliferation- and differentiation-inducing factors, such as colony stimulating factor 1 (CSF1) and enzymes involved in retinoic acid (RA) biosynthesis. We show that transient depletion of macrophages leads to a disruption in spermatogonial differentiation. These findings reveal an unexpected role for macrophages in the spermatogonial niche in the testis, and raise the possibility that macrophages play previously unappreciated roles in stem/progenitor cell regulation in other tissues.

Introduction

One of the most important biological functions of the adult testis is to maintain fertility over an extended reproductive lifespan by balancing renewal and differentiation divisions of spermatogonial stem cells (SSCs) inside seminiferous tubules. Defects in either self-renewal or differentiation of SSCs lead to depletion of sperm and infertility.

[*]**Corresponding Author:** Tony DeFalco, tony.defalco@cchmc.org, Division of Reproductive Sciences, Cincinnati Children's Hospital Medical Center, 3333 Burnet Avenue, MLC 7045, Cincinnati, OH 45229 USA, Phone: +1-513-803-3988, Fax: +1-513-803-1160.

Author Contributions

The authors have made the following contributions: Conceived and designed the experiments: TD BC. Performed the experiments: TD SJP AVW BW MJK. Analyzed the data: TD SJP BC. Wrote the paper: TD SJP BC.

In the prevailing model of the SSC hierarchy, the isolated, single spermatogonia, A_{single}, are the most undifferentiated cells in the lineage, some of which comprise the steady-state SSC population (Chan et al., 2014; de Rooij, 1973; Oakberg, 1956, 1971). The progeny of A_{single} cells undergo incomplete cytokinesis, giving rise to syncytial cysts of 2 (A_{paired}), 4 ($A_{aligned\text{-}4}$), 8 ($A_{aligned\text{-}8}$), or 16 ($A_{aligned\text{-}16}$) spermatogonia. These cells comprise the undifferentiated spermatogonia (A_{undiff}), and are located on the basement membrane of the seminiferous tubule interspersed among Sertoli cells, the somatic cell lineage within the tubule that supports spermatogenesis. Further differentiation of $A_{aligned}$ spermatogonia produces A1 ("differentiating") spermatogonia that, after multiple mitotic divisions, enter meiosis, undergo spermiogenesis, and proceed toward the tubule lumen.

The microenvironment that regulates stem cell self-renewal and differentiation divisions is referred to as the stem cell niche (Li and Xie, 2005). Unlike the well-defined and distally localized germline stem cell niche in the gonads of other model organisms, such as *Drosophila* and *C. elegans*, the mammalian testis contains many potential germline stem cell niches (in the range of several thousand to 40,000 per testis) (Shinohara et al., 2001; Tegelenbosch and de Rooij, 1993) that are not well characterized, but are believed to be randomly located along the tubules. In part because the SSC niche lacks a stereotypic location, it has proven difficult to define its cellular constituents in mammals.

Within the testis interstitium there are multiple cell types that influence the SSC niche directly or indirectly, including steroidogenic Leydig cells that produce testosterone, which is known to influence spermatogenesis (Smith and Walker, 2014), and peritubular myoid cells (PMCs) that encase seminiferous tubules, communicate directly with underlying Sertoli cells in the tubule, and provide structural support and peristaltic action. In addition, vascular endothelium with its associated perivascular cells is also associated with the surface of seminiferous tubules. Undifferentiated spermatogonia localize to regions of the seminiferous tubule that border the vascularized interstitial compartment (Yoshida et al., 2007). Thus, the endothelium or other cells typically associated with the vasculature may act to establish and maintain the niche.

Macrophages, which are frequently associated with vasculature, are present in large numbers in the adult testis interstitium (Hume et al., 1984). A growing number of non-immune functions have been attributed to macrophages in other tissues. For example, macrophages are involved in vascular development of the fetal brain (Fantin et al., 2010). In the juvenile and adult testis, macrophages are intimately associated with Leydig cells and promote steroidogenesis (Cohen et al., 1997; Gaytan et al., 1994; Hutson, 2006), although the mechanism through which this interaction is mediated is not entirely clear. Interestingly, genes involved in immune cell differentiation and chemotaxis, such as *Csf1r*, *Itgal*, *Ccl2*, *Ccl3*, *Ccl7*, *Cxcl2*, and *Cxcl4*, are enriched in the transcriptome of SSCs (Kokkinaki et al., 2009; Oatley et al., 2009), suggesting that communication between cells of the immune system (such as macrophages) and SSCs potentially plays an important role in spermatogenesis.

In this study, we investigated a role for macrophages in regulation of the spermatogonial progenitor niche in the testis. We demonstrate that a transient ablation of macrophages in the

adult testis does not affect SSC maintenance, but results in fewer spermatogonia, likely by affecting spermatogonial differentiation. We define unique populations of macrophages within the adult testis, one of which localizes along the surface of seminiferous tubules, spatially associates with spermatogonial precursors, and expresses spermatogonial proliferation- and differentiation-inducing molecules such as colony stimulating factor 1 (CSF1) and enzymes in the retinoic acid (RA) biosynthetic pathway. The effects observed on spermatogonial activity are consistent with local macrophage-spermatogonial interactions, and are likely independent of known macrophage functions in regulating steroidogenesis. This work demonstrates an unexpected role for macrophages in spermatogonial development and raises the possibility that macrophages play previously unappreciated roles in stem/progenitor cell regulation in other tissues.

Results

Testicular macrophages are located in both the interstitium and along the seminiferous tubules

To examine macrophage populations in the adult testis, we used well-characterized markers of the testicular macrophage lineage, such as F4/80 (Hume et al., 1984) and AIF1 (IBA1; (Kohler, 2007)). Macrophages in the interstitial compartment were intimately intermingled among Leydig cells (Figure 1A and 1A'), consistent with previous observations that macrophages and adult Leydig cells form unique intercellular contacts (Hutson, 1992). Macrophages were also intimately associated with interstitial testicular vasculature, and often extended long processes along the length of blood vessels within Leydig cell clusters (Figure 1B).

We examined the association of macrophages with lymphatic vessels. Consistent with previous reports (Hirai et al., 2012; Svingen et al., 2012), lymphatic vessels (as labeled by Neuropilin 2 [NRP2] and LYVE1) were only detected in the outer tunica of the testis; macrophages were numerous throughout the tunica layer and were often associated with both blood vessels and lymphatic vessels (Figures S1A and S1B).

In addition to well-characterized interstitially localized macrophages (Hume et al., 1984), F4/80 also labeled a population of cells on the surface of seminiferous tubules (Figures 1A' and 1C). These cells had long processes, spanning up to 100 μm, and a stellate, ramified appearance characteristic of both neurons and macrophages. We first speculated that these peritubular cells belonged to a neuroendocrine lineage. However, they did not stain positive for HSD3B1 (Figures 1A and C), or express the neural-associated markers TUBB3 (Tubulin, beta 3 class III; TUJ1), S100b, or Nestin (Figure S1C–E). In contrast, peritubular cells were positive for macrophage/microglial markers, such as AIF1, ITGAM (CD11b), F4/80, CD68, *Cx3cr1*-GFP (Jung et al., 2000), and *Mafb*-GFP (Moriguchi et al., 2006) (Figure 1C–E). These macrophages made extensive contacts with blood vessels extending over the tubule surface; most were closely associated with tubular vasculature, while some were independent (Figure 1F). Peritubular macrophages were intermingled with PMCs and formed rosette-like structures similar to those observed in the neural stem cell niche (Zhang et al., 2001) (Figures 1G and 1H).

Peritubular and interstitial macrophages showed unique expression of two myeloid-associated markers: CSF1R was expressed at low levels in peritubular cells but at high levels in interstitial macrophages, whereas the opposite was true for major histocompatibility complex II (MHCII) (Figure 1I); all other macrophage markers tested were clearly detected in both cell populations. Consistent with immunofluorescence results, flow cytometry revealed that there were at least 2 major subsets of testis macrophages: CSF1R–positive, MHCII-negative (interstitial macrophages) and CSF1R–negative, MHCII-positive (peritubular macrophages) (Figure 1J–N). These two populations were present in similar numbers in the testis (Figures 1M and 1N). Additionally, we observed a CSF1R and MHCII double-negative population, which may represent undifferentiated macrophages or a macrophage population that expressed only low levels of these cell-surface markers by flow cytometry (Figure 1M).

Peritubular macrophages are localized to the myoid layer immediately overlying spermatogonial precursors

Using the transcriptional repressor ZBTB16 (PLZF; (Buaas et al., 2004; Costoya et al., 2004)) as a marker for undifferentiated spermatogonia and A1-A3 differentiating spermatogonia in cryosections of adult testes, we found that the few ZBTB16-positive cells per section were often (but not always) adjacent to F4/80-positive macrophages (Figures 2A and 2A’). In analysis of whole-mount seminiferous tubules, a correlation between macrophage density along seminiferous tubules and the number of ZBTB16-positive cells in the tubule was evident (Figures 2B and 2C). Although the association of macrophages with undifferentiated spermatogonia was not absolute on a cell-by-cell basis, large groups of spermatogonia were consistently located in tubule regions enriched for macrophages, suggesting a relationship between the two populations.

3D reconstruction of seminiferous tubules revealed that macrophages were overlying the Collagen-IV-containing tubule basement membrane in the smooth muscle alpha actin (ACTA2, a-SMA)-positive PMC layer and did not appear to be penetrating deeply into the tubule (Figures S2A and S2B and Movie S1). However, macrophages were often in very close proximity to blood vessels and ZBTB16-positive cells (Figure S2C and Movie S2).

We found that the specification, recruitment, and localization of peritubular and interstitial macrophages were not dependent on *Cx3cr1*, as *Cx3cr1*-GFP homozygous mutant testes showed normal macrophage populations and testis function (Figure S2D–I), consistent with previous reports that these mutants are fertile (Jung et al., 2000).

Macrophage density along the seminiferous tubule increases at locations containing the highest concentration of undifferentiated spermatogonia

To investigate macrophage localization and its relationship to spermatogenesis, we utilized markers to identify early spermatogonia at different stages of the spermatogenic cycle. Two populations of ZBTB16-positive cells could be distinguished: bright and dim (Figure S3A). Using another marker of undifferentiated spermatogonia, Cadherin 1 (CDH1; E-cadherin) (Tokuda et al., 2007) and a marker of A1 differentiating spermatogonia and later stages, KIT (C-KIT) (Schrans-Stassen et al., 1999), we confirmed that ZBTB16-bright cells were A_{single},

A_{paired} and $A_{aligned\text{-}4,8,16}$ undifferentiated spermatogonia (Figure S3B), while long chains of ZBTB16-dim cells were A1-A3 differentiated spermatogonia (Figure S3C–E). While strongest expression of ZBTB16 is in undifferentiated and A1 spermatogonia, sensitive detection methods allow visualization of ZBTB16 also within A2 and A3 spermatogonia (Meistrich and Hess, 2013).

We grouped tubules into subsets of the cycle stages: stages I-V, VI-VII (in which the number of long ZBTB16-bright $A_{aligned}$ cysts reaches its peak), VIII-IX (in which A-type undifferentiated spermatogonia have transitioned into ZBTB16-dim A1 differentiating spermatogonia), and X-XII (in which A1 spermatogonia have become A2 and A3 spermatogonia, and there are low numbers of ZBTB16-bright cells and high numbers of ZBTB16-dim cells).

We found a significant increase in macrophage density along the tubule in stages VI-VII (Figure 2D), the stage in which the number of bright ZBTB16-positive undifferentiated spermatogonia is at its highest (Figure 2E), and a decrease in macrophage numbers as the cycle progressed away from stage VI-VII.

Induced diphtheria toxin receptor ablation is effective for depletion of testicular macrophages

To investigate whether macrophages regulate spermatogenesis, we ablated macrophages using the Cre-inducible diphtheria toxin receptor (iDTR) method (Buch et al., 2005) driven by *Cx3cr1*-Cre. GFP lineage tracing revealed that Cre expression was highly macrophage-specific in the testis (Figure S4A–F), as GFP was detected in ~95% of testicular F4/80- and AIF1-positive macrophages. Consistent with this observation, flow cytometry revealed that >95% of GFP-positive cells in *Cx3cr1*-GFP adult testes were F4/80- and CD11b/ITGAM-expressing macrophages (Fig. S4G).

We administered four doses of diphtheria toxin (DT) over the course of 7 days (Figures 3A and S4H) to eliminate macrophages and prevent their recovery from the systemic circulation. DT-treated *Cx3cr1*-Cre*;Rosa*-iDTR adult testes showed a significant overall reduction (>90%) in macrophages (Figures 3B–E and Figures S4I–L). Macrophage numbers in the testis recovered to about half of wild-type 4 days after the final DT injection, and fully recovered by 14 days (data not shown and Figures S5A and S5B). DT injection itself did not disturb short-term testis function, since testes from *Cx3cr1*-Cre-negative animals that were DT-injected were similar to wild-type testes in terms of macrophage populations and progression of spermatogenesis (Figures S5D and S5E).

Somatic Cell Types are Normal in Macrophage-Depleted Testes

After macrophage depletion, we found no evidence for increased apoptosis in the testis (Figures S4O and S4P), and found similar numbers of Sertoli cells as in controls. Sertoli cells were normal in morphology and expressed both SOX9 and GATA4 (Figures 3C, 3D, 3F, S4M, and S4N). In addition, vasculature (Figures S4M and S4N) and the Sertoli cell blood-testis barrier (as visualized by Claudin 11 staining; Figures S6A and S6B) were similar in control and macrophage-depleted testes.

We examined the effects of short-term adult macrophage ablation upon Leydig cells and testosterone (T) production (Cohen et al., 1996). The steroidogenic enzymes HSD3B1 (Figures S4K and S4L) and CYP17A1 (Figures S6C and S6D) were robustly expressed in macrophage-depleted samples by immunofluorescence, consistent with ongoing steroidogenesis. Measurements of T levels revealed that intratesticular T was reduced by ~50% ($P<0.01$) in macrophage-depleted samples relative to controls (Figure S6E). Any reductions in serum T levels were not statistically significant ($P>0.05$; Figure S6F). These findings suggest that Leydig cells were mildly affected but maintained basic functionality and testosterone production sufficient to support spermatogenesis during short-term macrophage depletion.

Macrophage-Depleted Testes Contain Fewer Spermatogonial Precursors

While most tubules in DT-treated *Cx3cr1*-Cre;*Rosa*-iDTR testes were completely devoid of F4/80-positive cells (>90% of tubules, group “DT b” in Figure 3), we occasionally found tubules with regions containing small numbers of macrophages (<10% of tubules, group “DT a” in Figure 3). These results were consistent with the expression pattern of the *Cx3cr1*-Cre (see above), which was approximately 95% efficient. We analyzed these groups of tubules separately for spermatogonial counts.

Staining of control and DT-treated whole-mount tubules revealed a 75% reduction in total ZBTB16-positive cells in macrophage-depleted testes (Figure 3G). While there was a 60% reduction in ZBTB16-bright cells (undifferentiated spermatogonia), ZBTB16-dim cells (A1-A3 differentiating spermatogonia) were more dramatically affected, with an 80% drop in numbers (from 13.1 to 2.6 cells per 10,000 εm^2 of tubule surface; Figure 3G). DT-treated tubules containing a few remaining macrophages (“DT a”) had a reduced number of ZBTB16-positive cells compared to control tubules, but had more ZBTB16-positive cells than tubules that were completely devoid of macrophages (Figures 3C, 3D. and 3G), consistent with the ability of an intermediate number of macrophages to sustain an intermediate level of spermatogenesis. These data suggest that loss of ZBTB16-positive cells is due to a local effect of ablating adjacent macrophages rather than a global, systemic defect such as disruption of T biosynthesis.

Long chains of CDH1-positive cysts that represent $A_{aligned}$ and A1-A3 cysts (see Figure S3), were rarely found in macrophage-depleted testes relative to DT-injected, Cre-negative controls (Figures 3H and 3I). A possible explanation for their absence is that differentiation of spermatogonia was disrupted. Consistent with this hypothesis, there was a reduction in the DDX4-(Mouse Vasa Homolog, MVH)-dim population of cells (containing spermatogonia and early-stage spermatocytes) (Fujiwara et al., 1994; Toyooka et al., 2000) near the basal lamina of macrophage-ablated tubules (Figures 3J and 3K).

The number of A_{single} and A_{paired} spermatogonial cysts was unaffected, while the number of long $A_{aligned}$ cysts was decreased (Figure 3L). These results suggest that, while SSCs were maintained, undifferentiated spermatogonia in macrophage-ablated tubules exhibited defects in differentiation. Long spermatogonial cysts reappeared after a 14-day recovery period (Figures S5A and S5C), indicating that SSCs persisted and could produce $A_{aligned}$ undifferentiated spermatogonia and A1-A3 differentiated spermatogonia again once

macrophages recolonized the testis. Consistent with normal SSC niche function, the SSC maintenance factor GDNF (Meng et al., 2000) was robustly expressed in Sertoli cells of macrophage-depleted testes (Figures S6G and S6H).

Cell Cycle Activity of Spermatogonial Precursors is Reduced in the Absence of Macrophages

To determine if the number of proliferative spermatogonia was altered in the absence of macrophages, we used a BrdU incorporation assay to label S-phase cells in control or macrophage-ablated testes. Comparison among tubules in wild-type controls revealed a positive correlation between numbers of BrdU-positive ZBTB16-expressing cells and numbers of macrophages on the surface of the tubule (Figures 4A–D and S7A–D). We found that 72% of total ZBTB16-positive cells were BrdU-positive in control samples, while only 52% of total ZBTB16-positive cells in DT-treated samples were BrdU-positive (Figure 4I).

Consistent with BrdU results, there was a reduced proportion of ZBTB16-expressing cells in active cell cycle after macrophage ablation. In control samples, 42% of bright ZBTB16-expressing cells (undifferentiated spermatogonia) stained positive for MKI67, a marker of active cell cycle, in contrast to only 30% in DT-treated samples (Figures 4E–F and 4I). Tubules in DT-treated testes adjacent to interstitial tissue where macrophages were still present contained increased numbers of MKI67/ZBTB16 double-positive spermatogonia as compared to regions where macrophages were completely depleted (Figures S7E and S7F). Consistent with this result, the cell cycle arrest marker CDKN1B (p27 or $p27^{kip1}$) was expressed in only 30% of bright ZBTB16 cells in controls compared to 62% in macrophage-depleted testes (Figures 4G–I), demonstrating a dramatic increase in of the percentage of quiescent undifferentiated spermatogonia. Overall, BrdU and cell cycle data are consistent with a role for macrophages in differentiation of spermatogonia: since there is a greater reduction of ZBTB16-dim differentiated A1-A3 cells (highly and rapidly proliferative) than ZBTB16-bright A_{single} and A_{paired} cells (with variable cell cycle activity and which are often quiescent during parts of the spermatogenic cycle), reduced expression of proliferation and active cell cycle markers would be anticipated as a secondary consequence of losing differentiated cell types.

Testicular macrophages express components of CSF1 and retinoic acid signaling pathways

To determine how macrophages potentially influence spermatogonial behavior, we analyzed two key signaling pathways involved in the progression of spermatogenesis: CSF1/CSF1R and retinoic acid (RA). Colony stimulating factor 1 receptor (CSF1R) is enriched in the SSC/undifferentiated spermatogonial population, and CSF1 promotes proliferation and/or self-renewal of ex vivo cultured spermatogonia (Kokkinaki et al., 2009; Oatley et al., 2009). CSF1/CSF1R signaling has traditionally been associated with recruitment and differentiation of monocytes and macrophages (Jones and Ricardo, 2013), so although Leydig cells and a subset of peritubular cells were reported to express CSF1 (Oatley et al., 2009), we examined CSF1 expression in macrophages. Using immunofluorescence, we found CSF1 expressed within both interstitial (vascular-associated) macrophages (Figure 5A) and peritubular

macrophages (Figure 5B). Anti-ACTA2 staining for peritubular myoid cells revealed that CSF1 was mostly localized to ACTA2-negative peritubular macrophages, but occasionally we observed weak CSF1 expression in myoid cells (Figure 5C). In addition, CSF1 staining localized to other cells associated with blood vessels that are negative for an endothelial-specific marker (PECAM1), but positive for a vascular-smooth-muscle-cell marker (ACTA2) (Figures 5A, 5D, and 5E). These data indicate that macrophages and vascular smooth muscle cells are both sources of CSF1 that could potentially influence adult spermatogonial behavior.

An important function of retinoic acid (RA) in the testis is to promote differentiation of spermatogonia and entry into meiosis. In RA-depleted testes (via dietary vitamin A depletion, genetic mutants for members of the RA biosynthesis pathway, or RA-synthesis-inhibiting drugs), germ cells throughout the testis are arrested at the undifferentiated spermatogonial stage (Amory et al., 2011; Brooks and van der Horst, 2003; Griswold et al., 1989; Li et al., 2011; Mitranond et al., 1979; Wolbach and Howe, 1925), similar to what we observe in macrophage-depleted testes. *Stra8*, a reporter for RA activity, is induced at stage VI of the spermatogenic cycle (Zhou et al., 2008), the stage at which macrophage density is highest along the testis tubules, further potentially implicating macrophages in RA signaling in the testis.

We found that two essential RA synthesis enzymes, ALDH1A2 (RALDH2) and RDH10, are expressed by testicular macrophages. Immunofluorescence revealed that ALDH1A2 was expressed in the interstitium of the adult testis, specifically in Leydig cells and in both interstitial and peritubular macrophages, but not within vasculature (Figures 6A and B); however, we found that expression in peritubular macrophages was much weaker than in interstitial macrophages (Figure 6C). ALDH1A2 expression was detected within meiotic and post-meiotic germ cells, as previously described (Vernet et al., 2006). *Rdh10* expression in Sertoli and germ cells is specifically required for juvenile spermatogenesis (Tong et al., 2013), but is not required for adult spermatogenesis, suggesting that there is another source of RDH10 in adult testes. Consistent with these findings, RDH10 is expressed broadly in the juvenile testis, similar to ALDH1A2: within Sertoli cells, germ cells, and interstitial cells (data not shown). However, by adult stages, testis RDH10 was excluded from Sertoli cells and restricted to peritubular macrophages as well as some interstitial macrophages (Figure 6D).

Expression of CSF1 and RA synthesis enzymes was perturbed in macrophage-depleted testes

CSF1 expression was diffuse and failed to be specifically localized within interstitial and perivascular regions in macrophage-depleted testes relative to wild type (Figures 7A and 7B), suggesting that expression or localization of CSF1 is dependent on the presence of macrophages. ALDH1A2 expression similarly was decreased within Leydig cell clusters relative to controls (Figures 7C and 7D), although expression of both these factors was relatively unchanged in meiotic and post-meiotic germ cells. RDH10 expression in the interstitium was almost completely absent in macrophage-depleted testes (Figures 7E and

7F), consistent with the absence of peritubular macrophages, the main source of this enzyme in the adult testis interstitium.

Discussion

Elucidation of the SSC niche in the mammalian testis has proven difficult. Although *Neurogenin3*-GFP undifferentiated spermatogonia are preferentially localized near highly vascularized interstitium (Yoshida et al., 2007), *Id4*-GFP-positive A_{single} cells are located in a niche that is avascular (Chan et al., 2014). An inclusive model can be envisioned in which a small subset of A_{single} cells localize to avascular regions, which constitute the SSC niche, but once committed to proliferation or differentiation A_{single} cells move to vascular and interstitial-associated regions to access requisite oxygen, metabolites, hormones, and growth factors.

The cell types in the interstitium that contribute to the spermatogonial niche are not well understood. While macrophages have been identified in the testis interstitium (Hume et al., 1984), their role in spermatogonial development has not been investigated. We show that macrophages localize along tubules in regions of high spermatogonial precursor cell density and affect the ability of undifferentiated spermatogonia to differentiate and proceed through spermatogenesis. These findings suggest that macrophages, independently or in communication with vasculature or other interstitial cell populations (such as Leydig cells and perivascular smooth muscle cells), influence the activity of the spermatogonial niche, likely (although not exclusively) through the regulation of CSF1 expression and RA synthesis.

Roles for Macrophages in the Spermatogonial Niche

The importance of vasculature as a component of the SSC niche (Yoshida et al., 2007) may be partially mediated by vascular-associated macrophages and their association with perivascular smooth muscle cells. CSF1, expressed by perivascular smooth muscle cells, has been proposed to act through CSF1R expressed in spermatogonia to promote both proliferation (Kokkinaki et al., 2009) and self-renewal (Oatley et al., 2009). Macrophages, which are in close spatial proximity to undifferentiated spermatogonia, also produce CSF1 and may be required for CSF1 expression from other cellular sources or for CSF1 localization (by sequestering CSF1 via CSF1R).

RA signaling is critical for the progression of spermatogenesis and requires the activity of biosynthetic enzymes, such as RDH10 and ALDH1A2. *Rdh10* expression in Sertoli and germ cells is critical for juvenile spermatogenesis, but spermatogenesis in Sertoli-cell-and-germ-cell *Rdh10* conditional mutant testes recovered in adulthood (Tong et al., 2013), suggesting an additional source of RDH10. A subset of macrophages, mostly localized to the surface of seminiferous tubules, expresses RDH10, and could potentially be the compensatory source of RA that rescued loss of Sertoli- and germ-cell-derived RA in the adult *Rdh10* conditional mutant testis. Production of ALDH1A2 in Leydig cells also was affected by loss of macrophages. This macrophage-Leydig cell interaction is similar to the dependence of steroid hormone production on macrophages (Gaytan et al., 1994; Hutson, 1992, 2006). Consistent with the dependence of interstitial RA production on the presence of

macrophages, macrophage-depleted testes exhibited early spermatogonial defects reminiscent of vitamin-A- and RA-synthesis-deficient animals.

Macrophages may mediate the physical organization of peritubular myoid cells in nichelike clusters, which may form an environment conducive to spermatogonial differentiation into A1 spermatogonia. Macrophages accumulate at maximum density at stages VI-VII, in parallel with peak numbers of ZBTB16-bright spermatogonia, and just prior to and during the stage when spermatogonial divisions give rise to long chains of ZBTB16-dim A1 differentiated spermatogonia. Macrophage depletion disrupts the differentiation of ZBTB16-bright cells, and blocks the accumulation of long chains of ZBTB16-dim cells. This suggests that macrophages are responsible for spermatogonial progression, at least from stage VI-VII to stage VIII. One possibility is that macrophages are recruited to the tubule by a signal gradient that reflects the density of spermatogonial precursors. Undifferentiated spermatogonia and macrophages express multiple cytokine/receptor pairs that could be involved in recruitment (Kokkinaki et al., 2009; Oatley et al., 2009). Whether or how macrophages regulate spermatogenic waves in the seminiferous epithelium remain open questions.

Other Roles of Macrophages in the Testis

Interstitial macrophages form intercytoplasmic digitations with Leydig cells and are required for Leydig cell function (Cohen et al., 1996; Cohen et al., 1997; Gaytan et al., 1994; Hutson, 2006), They secrete 25-hydroxycholesterol (an intermediate in the testosterone biosynthetic pathway) (Hutson, 1992; Nes et al., 2000), and may regulate the unique intracellular and mitochondrial ultrastructure within Leydig cells that is required for steroid biogenesis (Cohen et al., 1996; Cohen et al., 1997).

Testosterone is critical for the progression of spermatogenesis; androgen-receptor-deficient testes exhibit meiotic stage arrest of germ cells (De Gendt et al., 2004; Yeh et al., 2002). Our macrophage depletion system is driven by *Cx3cr1*-Cre; as *Cx3cr1* is also expressed in monocytes, dendritic cells, natural killer cells, yolk-sac-derived primitive macrophages, and brain microglia (DeFalco et al., 2014; Jung et al., 2000), it is formally possible that systemic loss of other immune cell types in the body could affect steroid production or testis function for other unknown reasons. A major concern would be depletion of microglia, which are required for brain-gonadal hormonal regulation (Cohen et al., 1996); however, our results from short-term macrophage depletion are not consistent with a simple defect in testosterone production. First, the undifferentiated spermatogonial defects we observed occur much earlier in spermatogenesis than the meiotic arrest typical of androgen depletion or androgen signaling disruption (Chang et al., 2004; De Gendt et al., 2004; Yeh et al., 2002). Second, functional levels of testosterone are still present in macrophage-depleted testes during the period of transient macrophage ablation. Leydig cells still robustly express the steroidogenic enzymes HSD3B1 and CYP17A1, and the levels of serum and intratesticular testosterone in short-term macrophage-depleted testes are well above the experimentally determined thresholds for quantitatively and qualitatively normal spermatogenesis in rats, which require <20% of control testosterone levels to sustain spermatogenesis (Awoniyi et al., 1989a; Awoniyi et al., 1989b; Zirkin et al., 1989). In addition, we detected an intact blood-testis

barrier, known to be heavily reliant on testosterone levels (Smith and Walker, 2014). Third, depletion of ZBTB16-positive cells along the tubule is not uniform (as would be predicted by a global, severe defect in steroidogenesis), but is highly correlated with regions of the tubule completely depleted of macrophages. All of this evidence suggests that perturbations of spermatogonial behavior we observed are not caused by loss of hormone biosynthesis. Instead, they are consistent with loss of local macrophage-spermatogonial interactions.

It may be important to understand whether peritubular macrophages communicate with interstitial macrophages surrounding vasculature and/or nests of Leydig cells. These macrophage populations may remain distinct and specialize in unique roles in testis biology (e.g., regulation of vascular and Leydig cells vs. regulation of spermatogonial differentiation). Alternatively, these populations could be interchangeable and/or communicate closely to regulate lifelong fertility. The expression pattern of MHCII suggests distinct immunological roles for different macrophage subsets, such as antigen-presenting activity by peritubular macrophages. The testis is a generally immune-privileged organ, due to the immunosuppressive function of Sertoli cells, androgen production by Leydig cells, and the presence of M2-like macrophages (Meinhardt and Hedger, 2011). However, in pathological or injury conditions it is possible that different macrophage populations possess unique immunological capabilities. Although we currently lack tools to assess the requirement of interstitial versus peritubular macrophages, future experiments may refine their roles.

Macrophages in Stem Cell Biology

The bone marrow is one of the few tissues described in which the presence of myeloid cells has been shown to be required for stem cell niche function. When macrophages are depleted in vivo, the hematopoietic stem cell (HSC) niche is affected and HSCs are mobilized into the blood (Winkler et al., 2010).

Our findings that testis macrophages influence the activity of the SSC niche suggest that macrophages may be more broadly important in regulating stem cell populations than previously supposed. The pairing of cytokine secretion from stem cells and recruitment of immune cells to stem-cell-enriched regions of tissues may be a conserved mechanism by which immune homeostasis can be linked to tissue repair and stem cell niches.

Experimental Procedures

Mice

CD-1 (Charles River), C57BL/6J (B6; Jackson Laboratories), and *Mafb*-GFP$^{+/-}$ (Moriguchi et al., 2006) mice (maintained on a B6 background), were used for wild-type expression studies. *Cx3cr1*-Cre mice (MW126-Cre; 129/B6 mixed background) were generated by the GENSAT project (Gong et al., 2003). *Cx3cr1*-GFP (Jung et al., 2000) (B6 or B6/CD-1 mixed background; this line is a knock-in loss-of-function mutation utilized as a heterozygous reporter unless specifically analyzed for homozygous mutation), *Rosa*-iDTR (Buch et al., 2005) (B6 background), and *Rosa*-tdTomato (Madisen et al., 2010) (B6 background) mice were obtained from Jackson Laboratories. Farnesylated-GFP reporter

mice (*Rosa26R–CAG-fGFP*) (Rawlins et al., 2009) are maintained on a B6 background. All mice used were approximately 3 months old, and were sacrificed via cervical dislocation or isoflurane administration followed by bilateral thoracotomy. Mice were housed in accordance with NIH guidelines, and experimental protocols were approved by the Institutional Animal Care and Use Committee of Duke University Medical Center or Cincinnati Children's Hospital Medical Center.

Cryosection Immunofluorescence

Whole testes were fixed in 4% paraformaldehyde (PFA) overnight at 4° C and processed for cryosection immunofluorescence as previously described (Defalco et al., 2013). Nuclei were stained with DAPI (Sigma) or Hoechst 33342 (Life Technologies), but all nuclear stains are listed as "DAPI". Samples were mounted in 2.5% DABCO (Sigma) in 80% glycerol or Fluoromount (Southern Biotech) and imaged on a Leica SP2 confocal microscope or Nikon EclipseTE2000-E microscope equipped with OptiGrid structured illumination imaging system running Phylum (Improvision) or Volocity (PerkinElmer) software. Primary antibodies used are listed in Table S1. Alexa-488-, Alexa-555-, and Alexa-647-conjugated secondary antibodies (Life Technologies/Molecular Probes) were all used at 1:500. Dy-Lite 488 donkey anti-chicken and Cy3 donkey or goat anti-rabbit/rat/mouse secondary antibodies (Jackson Immunoresearch) were used at 1:500.

Whole mount seminiferous tubule immunofluorescence and 3D reconstruction

Adult testes were de-capsulated and tubules were gently teased apart in PBS to remove interstitial cells. Tubules were fixed in 4% PFA containing 0.1% Triton X-100 rocking overnight at 4° C, and processed for immunofluorescence and imaging as described above. 3D images were acquired using the Nikon A1 confocal imaging system, which operates on NISElements software (Nikon; Tokyo, Japan). Images were spatially re-assembled using Z-stacks to generate a 3-dimensional representation from which single snapshots, orthogonal views, and movies were created.

Cell Counts

For ZBTB16, Sertoli cell (via SOX9), and macrophage (via F4/80) cell counts, 15–25 different random tubules of varying stages within each testis were used (n=3 testes). For BrdU experiments 35 tubules were used (n=3), while for MKI67 and CDKN1B analyses 15–20 different cryosections were used (n=3). To ensure that the entire depth of the seminiferous epithelium was included in whole-mount analyses, four separate Z-stacks were obtained for each tubule image (over a total depth of ~12 μm), which were then subjected to a maximum intensity projection. The surface area of an individual tubule within a 375 μm × 375 μm image (i.e., a single image taken with a 40× objective) was calculated by the Measure Function in Fiji/ImageJ (NIH). Cells were counted manually with Fiji's Cell Counter plug-in, and were normalized to a unit area of 10,000 μm^2. Bright versus dim ZBTB16 expression was verified using the Threshold function in Fiji. Graph results are shown as value ± SEM. Statistical analyses were performed using a two-tailed Student's t-test.

Diphtheria Toxin Injections

Diphtheria toxin (DT) (List Biologicals) was diluted in PBS at a concentration of 10 μg/ml. One μg (100 μl) of DT was injected intraperitoneally (i.p.) into *Cx3cr1*-Cre/+; *Rosa*-iDTR/+ mice (n=6) every other day for 7 days. Testes were isolated 24–72 hours after final injection. *Cx3cr1*-Cre/+;*Rosa*-iDTR/+ PBS-injected mice, +/+;*Rosa*-iDTR/+ DT-injected mice, or B6 uninjected mice served as controls (n=7).

BrdU Studies

Three-month old B6 control (n=4) or macrophage-depleted mice (n=4) were injected i.p. with 1.5 mg 5-bromo-2'-deoxyuridine (BrdU; Sigma) dissolved in 7 mM NaOH/PBS. Injections were performed 5 hours before sacrifice and removal of testes. Fixation and antibody staining were done as described as above; for BrdU staining samples were treated for 30 minutes in 2N HCl prior to blocking and addition of anti-BrdU primary antibody.

Hormone measurements

Testosterone measurements were performed by the University of Virginia Center for Research in Reproduction Ligand Assay and Analysis Core. Whole adult testes were mechanically lysed, and supernatant was collected. Sera were collected as described on the Ligand Assay and Analysis Core website (http://www.medicine.virginia.edu/research/institutes-and-programs/crr/lab-facilities/sampleprocessingandstorage-page).

Flow cytometry

Decapsulated CD-1 or *Cx3cr1*-GFP adult testes were dissociated by incubating at 37° C in a 250-rpm shaker for 20 minutes in a disassociation solution (PBS containing 0.5 mg/mL Collagenase Type 1 (Worthington; #LS004194), 0.5 mg/mL Collagenase Type 4 (Worthington; #LS004186), and 4μl/mL DNase I (Promega; #M6101)). Supernatant was pelleted, washed with PBS, and incubated in ACK buffer (Life Technologies; #A10492-01) for 5 minutes at room temperature to lyse erythrocytes. Cell suspensions were washed twice with PBS and filtered through a cell strainer cap (Falcon/Corning Life Sciences; #352235). For viability staining, cells were incubated prior to antibody incubation with Zombie Yellow Fixable Viability Kit (BioLegend; #423103) for 30 minutes in PBS. Cells were incubated with antibodies (Table S1) for 30 minutes in 1% heat-inactivated fetal bovine serum (FBS; Atlantic Biologicals; #S11510) in PBS containing 10% Fc Block (2.4G2 hybridoma supernatant), washed, and flow cytometry was performed on a BD Biosciences Fortessa I or Fortessa II flow cytometer. Prior to gating via CD45, cells were initially pre-gated via viability staining and singlet profiling. All data were analyzed using FlowJo (Treestar). Data is from two separate experiments on separate or pooled testes from two adult males.

Supplementary Material

Refer to Web version on PubMed Central for supplementary material.

Acknowledgments

We thank: M.D. Gunn for *Cx3cr1*-Cre, *Cx3cr1*-GFP, and *Rosa*-iDTR mice; F. Wang for *Rosa26R-CAG-fGFP* mice; S. Takahashi for *Mafb*-GFP mice; K. Morohashi and G. Enders for antibodies; I. Batchvarov and B. Kang for

technical assistance; M. Kofron and M. Muntifering at the Cincinnati Children's Hospital Medical Center (CCHMC) Confocal Imaging Core; and the Research Flow Cytometry Core in the Division of Rheumatology at CCHMC, supported in part by NIH AR-47363, NIH DK78392 and NIH DK90971. This work was funded by NIH grant 5R01-HD039963-13 and March of Dimes grant 1-FY10-355 to BC, and by NIH grant #1 F32 HD058433-01, a CCHMC Research Innovation and Pilot Funding Grant, a CCHMC Trustee Grant Award, CCHMC developmental funds, and a March of Dimes Basil O'Connor Starter Scholar Award (#5-FY14-32) to TD. SJP was supported by a CancerFree KIDS Research Grant.

References

Amory JK, Muller CH, Shimshoni JA, Isoherranen N, Paik J, Moreb JS, Amory DW Sr, Evanoff R, Goldstein AS, Griswold MD. Suppression of spermatogenesis by bisdichloroacetyldiamines is mediated by inhibition of testicular retinoic acid biosynthesis. J. Androl. 2011; 32:111–119. [PubMed: 20705791]

Awoniyi CA, Santulli R, Chandrashekar V, Schanbacher BD, Zirkin BR. Quantitative restoration of advanced spermatogenic cells in adult male rats made azoospermic by active immunization against luteinizing hormone or gonadotropin-releasing hormone. Endocrinology. 1989a; 125:1303–1309. [PubMed: 2667955]

Awoniyi CA, Santulli R, Sprando RL, Ewing LL, Zirkin BR. Restoration of advanced spermatogenic cells in the experimentally regressed rat testis: quantitative relationship to testosterone concentration within the testis. Endocrinology. 1989b; 124:1217–1223. [PubMed: 2492923]

Brooks NL, van der Horst G. Short-term effects of N'N-bis(dichloroacetyl)-1,8-octamethylenediamine (WIN 18446) on the testes, selected sperm parameters and fertility of male CBA mice. Lab. Anim. 2003; 37:363–373. [PubMed: 14599310]

Buaas FW, Kirsh AL, Sharma M, McLean DJ, Morris JL, Griswold MD, de Rooij DG, Braun RE. Plzf is required in adult male germ cells for stem cell self-renewal. Nat. Genet. 2004; 36:647–652. [PubMed: 15156142]

Buch T, Heppner FL, Tertilt C, Heinen TJ, Kremer M, Wunderlich FT, Jung S, Waisman A. A Cre-inducible diphtheria toxin receptor mediates cell lineage ablation after toxin administration. Nat. Methods. 2005; 2:419–426. [PubMed: 15908920]

Chan F, Oatley MJ, Kaucher AV, Yang QE, Bieberich CJ, Shashikant CS, Oatley JM. Functional and molecular features of the Id4+ germline stem cell population in mouse testes. Genes Dev. 2014; 28:1351–1362. [PubMed: 24939937]

Chang C, Chen YT, Yeh SD, Xu Q, Wang RS, Guillou F, Lardy H, Yeh S. Infertility with defective spermatogenesis and hypotestosteronemia in male mice lacking the androgen receptor in Sertoli cells. Proc. Natl. Acad. Sci. U.S.A. 2004; 101:6876–6881. [PubMed: 15107499]

Cohen PE, Chisholm O, Arceci RJ, Stanley ER, Pollard JW. Absence of colony-stimulating factor-1 in osteopetrotic ($csfm^{op}/csfm^{op}$) mice results in male fertility defects. Biol. Reprod. 1996; 55:310–317. [PubMed: 8828834]

Cohen PE, Hardy MP, Pollard JW. Colony-stimulating factor-1 plays a major role in the development of reproductive function in male mice. Mol. Endocrinol. 1997; 11:1636–1650. [PubMed: 9328346]

Costoya JA, Hobbs RM, Barna M, Cattoretti G, Manova K, Sukhwani M, Orwig KE, Wolgemuth DJ, Pandolfi PP. Essential role of Plzf in maintenance of spermatogonial stem cells. Nat. Genet. 2004; 36:653–659. [PubMed: 15156143]

De Gendt K, Swinnen JV, Saunders PT, Schoonjans L, Dewerchin M, Devos A, Tan K, Atanassova N, Claessens F, Lecureuil C, et al. A Sertoli cell-selective knockout of the androgen receptor causes spermatogenic arrest in meiosis. Proc. Natl. Acad. Sci. U.S.A. 2004; 101:1327–1332. [PubMed: 14745012]

de Rooij DG. Spermatogonial stem cell renewal in the mouse. I. Normal situation. Cell Tissue Kinet. 1973; 6:281–287. [PubMed: 4735543]

DeFalco T, Bhattacharya I, Williams AV, Sams DM, Capel B. Yolk-sac-derived macrophages regulate fetal testis vascularization and morphogenesis. Proc. Natl. Acad. Sci. U.S.A. 2014; 111:E2384–E2393. [PubMed: 24912173]

Defalco T, Saraswathula A, Briot A, Iruela-Arispe ML, Capel B. Testosterone levels influence mouse fetal leydig cell progenitors through notch signaling. Biol. Reprod. 2013; 88:91. [PubMed: 23467742]

Fantin A, Vieira JM, Gestri G, Denti L, Schwarz Q, Prykhozhij S, Peri F, Wilson SW, Ruhrberg C. Tissue macrophages act as cellular chaperones for vascular anastomosis downstream of VEGF-mediated endothelial tip cell induction. Blood. 2010; 116:829–840. [PubMed: 20404134]

Fujiwara Y, Komiya T, Kawabata H, Sato M, Fujimoto H, Furusawa M, Noce T. Isolation of a DEAD-family protein gene that encodes a murine homolog of Drosophila vasa and its specific expression in germ cell lineage. Proc. Natl. Acad. Sci. U.S.A. 1994; 91:12258–12262. [PubMed: 7991615]

Gaytan F, Bellido C, Aguilar E, van Rooijen N. Requirement for testicular macrophages in Leydig cell proliferation and differentiation during prepubertal development in rats. J. Reprod. Fertil. 1994; 102:393–399. [PubMed: 7861393]

Gong S, Zheng C, Doughty ML, Losos K, Didkovsky N, Schambra UB, Nowak NJ, Joyner A, Leblanc G, Hatten ME, et al. A gene expression atlas of the central nervous system based on bacterial artificial chromosomes. Nature. 2003; 425:917–925. [PubMed: 14586460]

Griswold MD, Bishop PD, Kim KH, Ping R, Siiteri JE, Morales C. Function of vitamin A in normal and synchronized seminiferous tubules. Ann. N.Y. Acad. Sci. 1989; 564:154–172. [PubMed: 2672955]

Hirai S, Naito M, Terayama H, Qu N, Kuerban M, Musha M, Ikeda A, Miura M, Itoh M. The origin of lymphatic capillaries in murine testes. J. Androl. 2012; 33:745–751. [PubMed: 22052776]

Hume DA, Halpin D, Charlton H, Gordon S. The mononuclear phagocyte system of the mouse defined by immunohistochemical localization of antigen F4/80: macrophages of endocrine organs. Proc. Natl. Acad. Sci. U.S.A. 1984; 81:4174–4177. [PubMed: 6377311]

Hutson JC. Development of cytoplasmic digitations between Leydig cells and testicular macrophages of the rat. Cell Tissue Res. 1992; 267:385–389. [PubMed: 1600565]

Hutson JC. Physiologic interactions between macrophages and Leydig cells. Exp. Biol. Med. (Maywood). 2006; 231:1–7. [PubMed: 16380639]

Jones CV, Ricardo SD. Macrophages and CSF-1: implications for development and beyond. Organogenesis. 2013; 9:249–260. [PubMed: 23974218]

Jung S, Aliberti J, Graemmel P, Sunshine MJ, Kreutzberg GW, Sher A, Littman DR. Analysis of fractalkine receptor CX(3)CR1 function by targeted deletion and green fluorescent protein reporter gene insertion. Mol. Cell. Biol. 2000; 20:4106–4114. [PubMed: 10805752]

Kohler C. Allograft inflammatory factor-1/Ionized calcium-binding adapter molecule 1 is specifically expressed by most subpopulations of macrophages and spermatids in testis. Cell Tissue Res. 2007; 330:291–302. [PubMed: 17874251]

Kokkinaki M, Lee TL, He Z, Jiang J, Golestaneh N, Hofmann MC, Chan WY, Dym M. The molecular signature of spermatogonial stem/progenitor cells in the 6-day-old mouse testis. Biol. Reprod. 2009; 80:707–717. [PubMed: 19109221]

Li H, Palczewski K, Baehr W, Clagett-Dame M. Vitamin A deficiency results in meiotic failure and accumulation of undifferentiated spermatogonia in prepubertal mouse testis. Biol. Reprod. 2011; 84:336–341. [PubMed: 20881313]

Li L, Xie T. Stem cell niche: structure and function. Annu. Rev. Cell Dev. Biol. 2005; 21:605–631. [PubMed: 16212509]

Madisen L, Zwingman TA, Sunkin SM, Oh SW, Zariwala HA, Gu H, Ng LL, Palmiter RD, Hawrylycz MJ, Jones AR, et al. A robust and high-throughput Cre reporting and characterization system for the whole mouse brain. Nat. Neurosci. 2010; 13:133–140. [PubMed: 20023653]

Meinhardt A, Hedger MP. Immunological, paracrine and endocrine aspects of testicular immune privilege. Mol. Cell. Endocrinol. 2011; 335:60–68. [PubMed: 20363290]

Meistrich ML, Hess RA. Assessment of spermatogenesis through staging of seminiferous tubules. Methods Mol. Biol. 2013; 927:299–307. [PubMed: 22992924]

Meng X, Lindahl M, Hyvonen ME, Parvinen M, de Rooij DG, Hess MW, Raatikainen-Ahokas A, Sainio K, Rauvala H, Lakso M, et al. Regulation of cell fate decision of undifferentiated spermatogonia by GDNF. Science. 2000; 287:1489–1493. [PubMed: 10688798]

Mitranond V, Sobhon P, Tosukhowong P, Chindaduangrat W. Cytological changes in the testes of vitamin-A-deficient rats. I. Quantitation of germinal cells in the seminiferous tubules. Acta Anat. (Basel). 1979; 103:159–168. [PubMed: 419926]

Moriguchi T, Hamada M, Morito N, Terunuma T, Hasegawa K, Zhang C, Yokomizo T, Esaki R, Kuroda E, Yoh K, et al. MafB is essential for renal development and F4/80 expression in macrophages. Mol. Cell. Biol. 2006; 26:5715–5727. [PubMed: 16847325]

Nes WD, Lukyanenko YO, Jia ZH, Quideau S, Howald WN, Pratum TK, West RR, Hutson JC. Identification of the lipophilic factor produced by macrophages that stimulates steroidogenesis. Endocrinology. 2000; 141:953–958. [PubMed: 10698170]

Oakberg EF. Duration of spermatogenesis in the mouse and timing of stages of the cycle of the seminiferous epithelium. Am. J. Anat. 1956; 99:507–516. [PubMed: 13402729]

Oakberg EF. Spermatogonial stem-cell renewal in the mouse. Anat. Rec. (Hoboken). 1971; 169:515–531.

Oatley JM, Oatley MJ, Avarbock MR, Tobias JW, Brinster RL. Colony stimulating factor 1 is an extrinsic stimulator of mouse spermatogonial stem cell self-renewal. Development. 2009; 136:1191–1199. [PubMed: 19270176]

Rawlins EL, Okubo T, Xue Y, Brass DM, Auten RL, Hasegawa H, Wang F, Hogan BL. The role of Scgb1a1+ Clara cells in the long-term maintenance and repair of lung airway, but not alveolar, epithelium. Cell Stem Cell. 2009; 4:525–534. [PubMed: 19497281]

Schrans-Stassen BH, van de Kant HJ, de Rooij DG, van Pelt AM. Differential expression of c-kit in mouse undifferentiated and differentiating type A spermatogonia. Endocrinology. 1999; 140:5894–5900. [PubMed: 10579355]

Shinohara T, Orwig KE, Avarbock MR, Brinster RL. Remodeling of the postnatal mouse testis is accompanied by dramatic changes in stem cell number and niche accessibility. Proc. Natl. Acad. Sci. U.S.A. 2001; 98:6186–6191. [PubMed: 11371640]

Smith LB, Walker WH. The regulation of spermatogenesis by androgens. Semin. Cell Dev. Biol. 2014; 30:2–13. [PubMed: 24598768]

Svingen T, Francois M, Wilhelm D, Koopman P. Three-dimensional imaging of Prox1-EGFP transgenic mouse gonads reveals divergent modes of lymphangiogenesis in the testis and ovary. PLoS One. 2012; 7:e52620. [PubMed: 23285114]

Tegelenbosch RA, de Rooij DG. A quantitative study of spermatogonial multiplication and stem cell renewal in the C3H/101 F1 hybrid mouse. Mutat. Res. 1993; 290:193–200. [PubMed: 7694110]

Tokuda M, Kadokawa Y, Kurahashi H, Marunouchi T. CDH1 is a specific marker for undifferentiated spermatogonia in mouse testes. Biol. Reprod. 2007; 76:130–141. [PubMed: 17035642]

Tong MH, Yang QE, Davis JC, Griswold MD. Retinol dehydrogenase 10 is indispensible for spermatogenesis in juvenile males. Proc. Natl. Acad. Sci. U.S.A. 2013; 110:543–548. [PubMed: 23267101]

Toyooka Y, Tsunekawa N, Takahashi Y, Matsui Y, Satoh M, Noce T. Expression and intracellular localization of mouse Vasa-homologue protein during germ cell development. Mech. Dev. 2000; 93:139–149. [PubMed: 10781947]

Vernet N, Dennefeld C, Rochette-Egly C, Oulad-Abdelghani M, Chambon P, Ghyselinck NB, Mark M. Retinoic acid metabolism and signaling pathways in the adult and developing mouse testis. Endocrinology. 2006; 147:96–110. [PubMed: 16210368]

Winkler IG, Sims NA, Pettit AR, Barbier V, Nowlan B, Helwani F, Poulton IJ, van Rooijen N, Alexander KA, Raggatt LJ, et al. Bone marrow macrophages maintain hematopoietic stem cell (HSC) niches and their depletion mobilizes HSCs. Blood. 2010; 116:4815–4828. [PubMed: 20713966]

Wolbach SB, Howe PR. Tissue Changes Following Deprivation of Fat-Soluble a Vitamin. J. Exp. Med. 1925; 42:753–777. [PubMed: 19869087]

Yeh S, Tsai MY, Xu Q, Mu XM, Lardy H, Huang KE, Lin H, Yeh SD, Altuwaijri S, Zhou X, et al. Generation and characterization of androgen receptor knockout (ARKO) mice: an in vivo model for the study of androgen functions in selective tissues. Proc. Natl. Acad. Sci. U.S.A. 2002; 99:13498–13503. [PubMed: 12370412]

Yoshida S, Sukeno M, Nabeshima Y. A vasculature-associated niche for undifferentiated spermatogonia in the mouse testis. Science. 2007; 317:1722–1726. [PubMed: 17823316]

Zhang SC, Wernig M, Duncan ID, Brustle O, Thomson JA. In vitro differentiation of transplantable neural precursors from human embryonic stem cells. Nat. Biotechnol. 2001; 19:1129–1133. [PubMed: 11731781]

Zhou Q, Nie R, Li Y, Friel P, Mitchell D, Hess RA, Small C, Griswold MD. Expression of stimulated by retinoic acid gene 8 (Stra8) in spermatogenic cells induced by retinoic acid: an in vivo study in vitamin A-sufficient postnatal murine testes. Biol. Reprod. 2008; 79:35–42. [PubMed: 18322276]

Zirkin BR, Santulli R, Awoniyi CA, Ewing LL. Maintenance of advanced spermatogenic cells in the adult rat testis: quantitative relationship to testosterone concentration within the testis. Endocrinology. 1989; 124:3043–3049. [PubMed: 2498065]

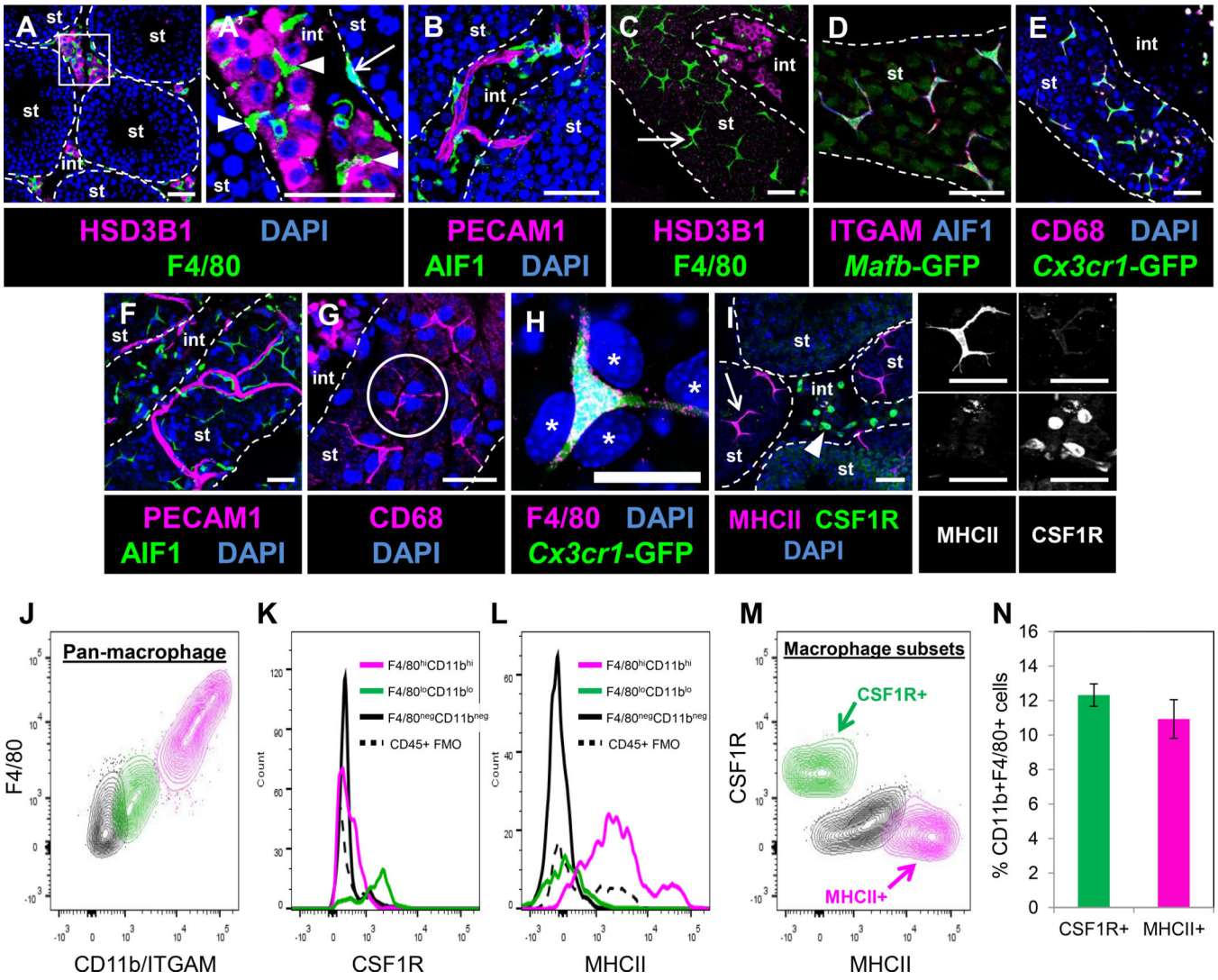

Figure 1. Adult testis macrophages are localized near Leydig cells, vasculature, and within the peritubular myoid cell layer

A' is a higher magnification of the boxed region in A. Dashed lines indicate outline of seminiferous tubules ("st") throughout all figures; "int" refers to interstitium throughout all figures. (A, A') Macrophages (arrowheads in A') were observed within clusters of HSD3B1-positive Leydig cells and overlying seminiferous tubule surfaces (arrow in A'). (B) Macrophages were associated with interstitial vasculature (marked with PECAM1). Peritubular cells (C, arrow) were positive for macrophage markers F4/80, ITGAM (CD11b), AIF1, *Mafb*-GFP, CD68, and *Cx3cr1*-GFP (C–E). Macrophages were in close proximity to tubular vasculature (F), and made rosette-like structures (G, circle outline) with tubule surface PMCs (large nuclei, asterisks in H). Peritubular (I, arrow) and interstitial (I, arrowhead) macrophages showed opposite expression patterns for MHCII and CSF1R. Black-and-white panels to the right of I are MHCII-only and CSF1R–only images for macrophages denoted in I. Thin scale bar, 50 μm; thick scale bar, 25 μm. Panels A and I are images from cryosectioned testes; remaining images are from whole-mount seminiferous tubules. Image in I is from a superficial cryosection that contains peritubular macrophages

overlying tubules (i.e., macrophages may appear to be but are not actually inside tubules); vasculature in B and F is overlying the tubule and is not within the tubule itself. (J) Flow cytometry of CD45+ cells from adult testis. Two populations of F4/80+CD11b/ITGAM+ macrophages (green and pink) are observed (black population represents CD45+ non-macrophage cell types). Histograms show differential expression of CSF1R (K) and MHCII (L) in corresponding color-coded populations from J; solid black lines in K and L represent CD45+ non-macrophage cells and dashed black lines in K and L represent fluorescence minus one (FMO) controls for total CD45+ cells. Contour plot in M shows CSF1R and MHCII expression in macrophage populations; black population represents double-negative population. Plots in J-M are representative experiments of four separate testes from two different CD-1 mice. Graph in N shows CSF1R+ and MHCII+ cells as a percent of total macrophages; gating is based on corresponding FMO control. Data in N are shown as mean ± SEM. See also Figures S1 and S2 and Movies S1 and S2.

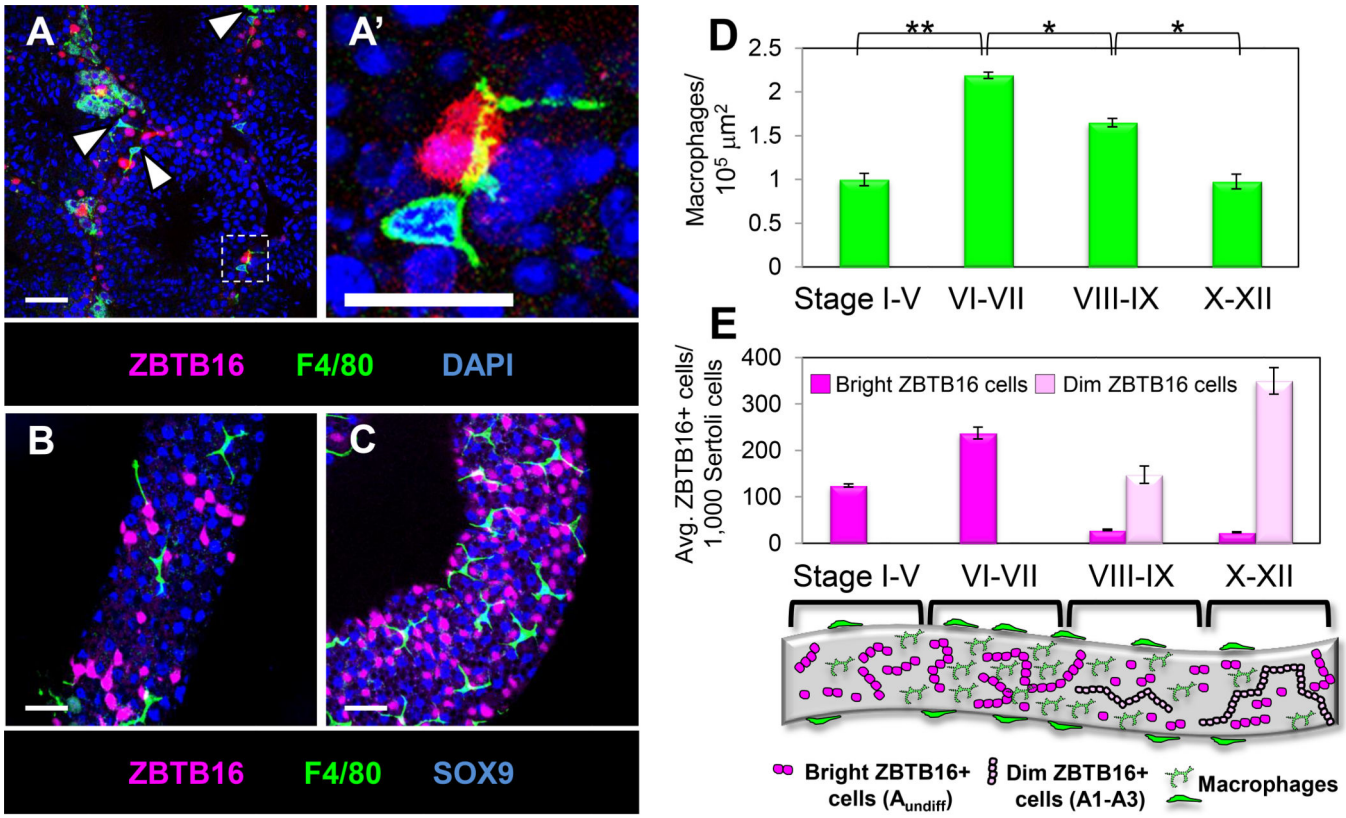

Figure 2. Macrophages are associated with regions of the seminiferous tubule containing ZBTB16-expressing undifferentiated spermatogonia

Immunofluorescence images of adult cryosectioned testis (A) and whole-mount seminiferous tubules (B, C). A' is a higher magnification of the boxed region in A. Macrophages (A, arrowheads) were located adjacent to ZBTB16-expressing cells and extended long cellular processes (A') over ZBTB16-positive cells. Tubule regions populated by fewer macrophages (B) had fewer ZBTB16-positive cells, as compared to high-density macrophage regions (C). Thin scale bar, 50 µm; thick scale bar, 25 µm. (D) Counts of macrophages per unit area for tubule regions of various stages of the spermatogenic cycle. *, $P<0.01$, **, $P<0.001$. (E) Counts of ZBTB16-bright and ZBTB16-dim cells at various stages of the spermatogenic cycle. Data are represented as mean ± SEM. Cartoon depicts stages of the spermatogenic cycle and representative numbers of ZBTB16-bright and ZBTB16-dim spermatogonia relative to macrophages along the tubule surface. See also Figure S3.

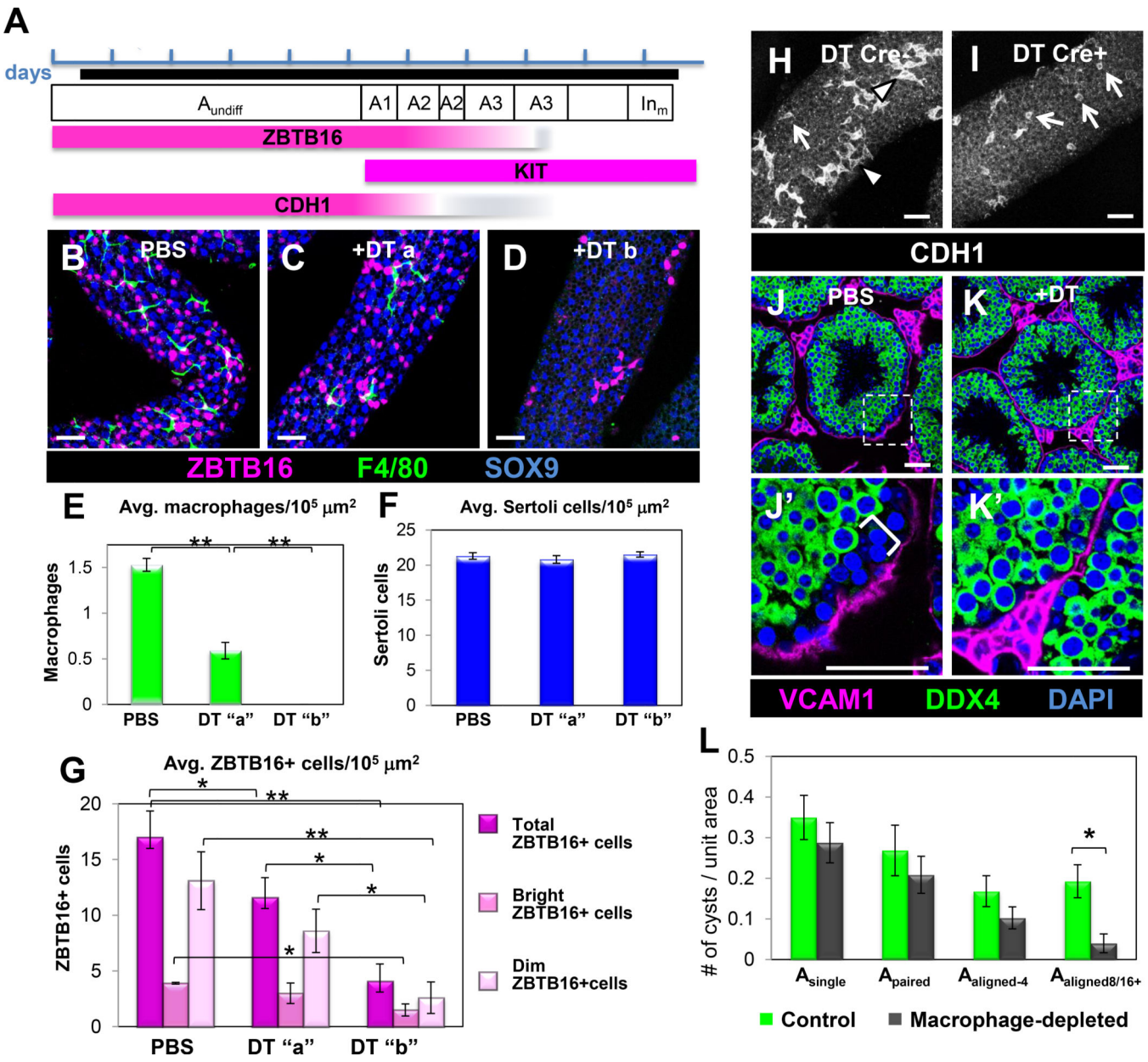

Figure 3. Ablation of macrophages results in decreased numbers of spermatogonia

(A) Timeline of the multiple-DT-injection scheme. Each blue bracket represents one day; macrophage depletion period is shown by a black line. DT injections were administered on days 1, 3, 5, and 7. Testes were harvested 24-72 hours after last injection. The mouse spermatogenic cycle is depicted, from A-type undifferentiated spermatogonia (A_{undiff}) to intermediate (mitosis) differentiated spermatogonia (In_m). Expression of stage-specific spermatogonial markers is shown below. (B) Control PBS-injected tubule. (C) "DT a" tubule. Group "DT a" denotes a minority of tubules (<10%) containing small numbers of macrophages. (D) "DT b" tubule. Group "DT b" denotes the majority of tubules (>90%) completely devoid of macrophages. SOX9 labels Sertoli cells. (E–G) Graphs show extent of macrophage ablation (E), Sertoli cell number (F), and total ZBTB16, ZBTB16-bright and

ZBTB16-dim cell number (G). Data are represented as mean ± SEM. *, $P<0.05$; **, $P<0.005$. (H, I) Control Cre-negative samples had a greater percentage of CDH1-positive long $A_{aligned}$ chains (H, arrowheads), whereas macrophage-depleted samples were biased towards shorter chains (H, I, arrows). (J, K) Macrophage-depleted testes showed a reduction in the basal-most population negative for DDX4 (bracket in J'); VCAM1 labels myoid cells overlying seminiferous tubules and labels interstitial cells. J' and K' are higher magnifications of the boxed regions in J and K, respectively. Scale bar, 50 mm. Panels B-D and H-I are from whole-mount seminiferous tubules; J-K are from cryosectioned testes. Graph in L shows numbers of different spermatogonial types (as defined by interconnected CDH1-expressing cells) per unit area. Data are represented as mean ± SEM. *, $P<0.01$. See also Figures S4–S6.

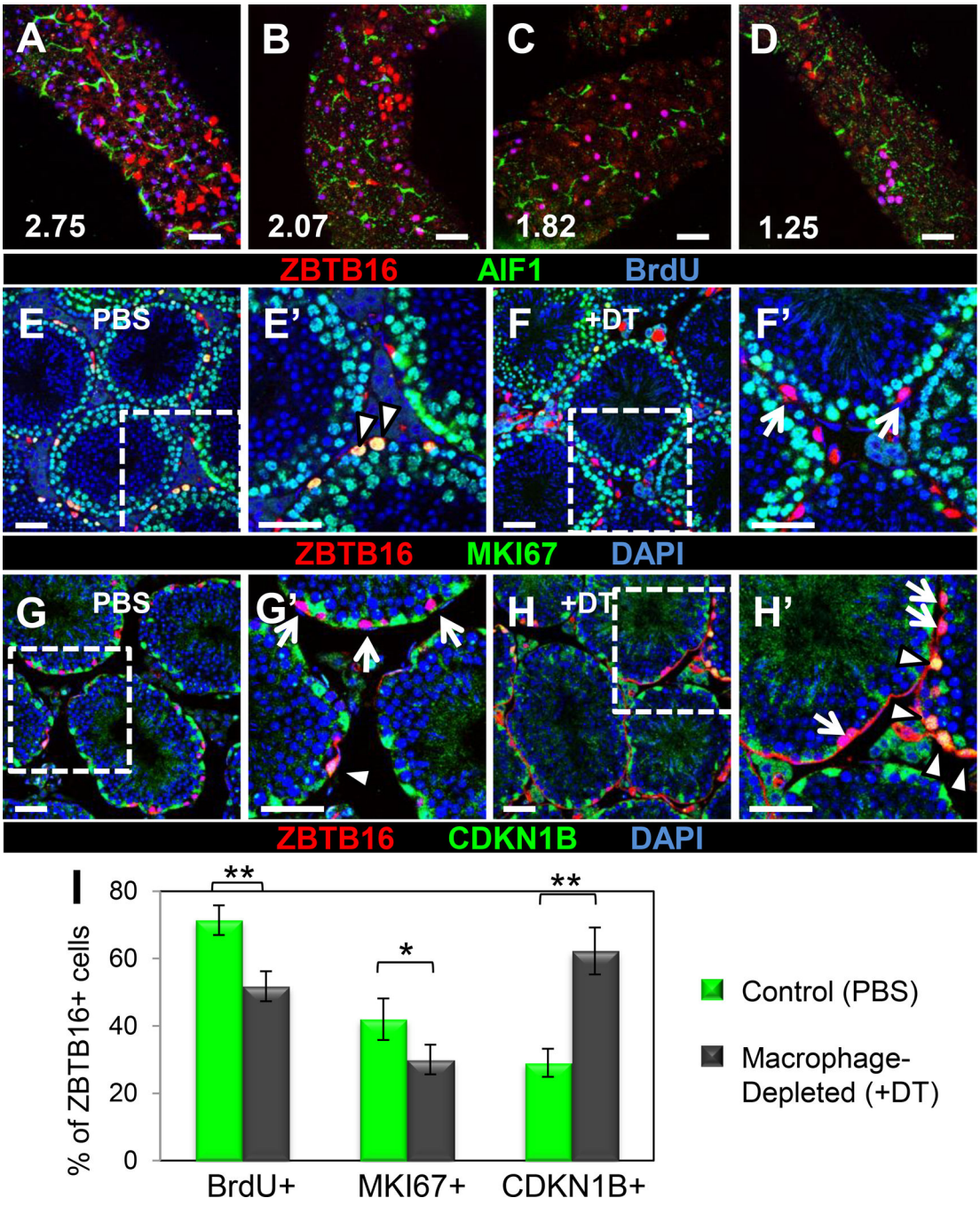

Figure 4. Depletion of macrophages leads to reduced cell cycle activity in undifferentiated spermatogonia

(A–D) Tubule regions with a higher density of macrophages (A, B) contained more proliferative cells than those with fewer macrophages (C, D); magenta-colored cells are ZBTB16 (red)/BrdU (blue) double-positive cells (i.e., proliferative spermatogonia). Number indicates macrophages per 10,000 μm^2 of seminiferous tubule surface area within frame of image. Control samples had a greater percentage of MKI67-positive ZBTB16-positive cells (E', arrowheads), whereas DT-treated samples had a higher percentage of MKI67-negative ZBTB16-positive cells (F', arrows). DT-treated testes contained an increased percentage of

quiescent CDKN1B–positive ZBTB16 cells (G', H', arrowheads) relative to non-quiescent ZBTB16 cells (G', H', arrows). E'-H' are higher magnifications of the boxes in E-H, respectively. Scale bar, 50 εm. (I) Graph showing reduced numbers of proliferative cells (BrdU+) among all ZBTB16- positive cells, reduced active cell cycle status (MKI67+) within ZBTB16-bright cells, and increased quiescence (CDKN1B+) within ZBTB16-bright cells. Data are represented as mean percentage ± SEM. *, $P<.05$; **, $P<.005$. Panels A-D are from whole-mount seminiferous tubules; E-H are from cryosectioned testes. See also Figure S7.

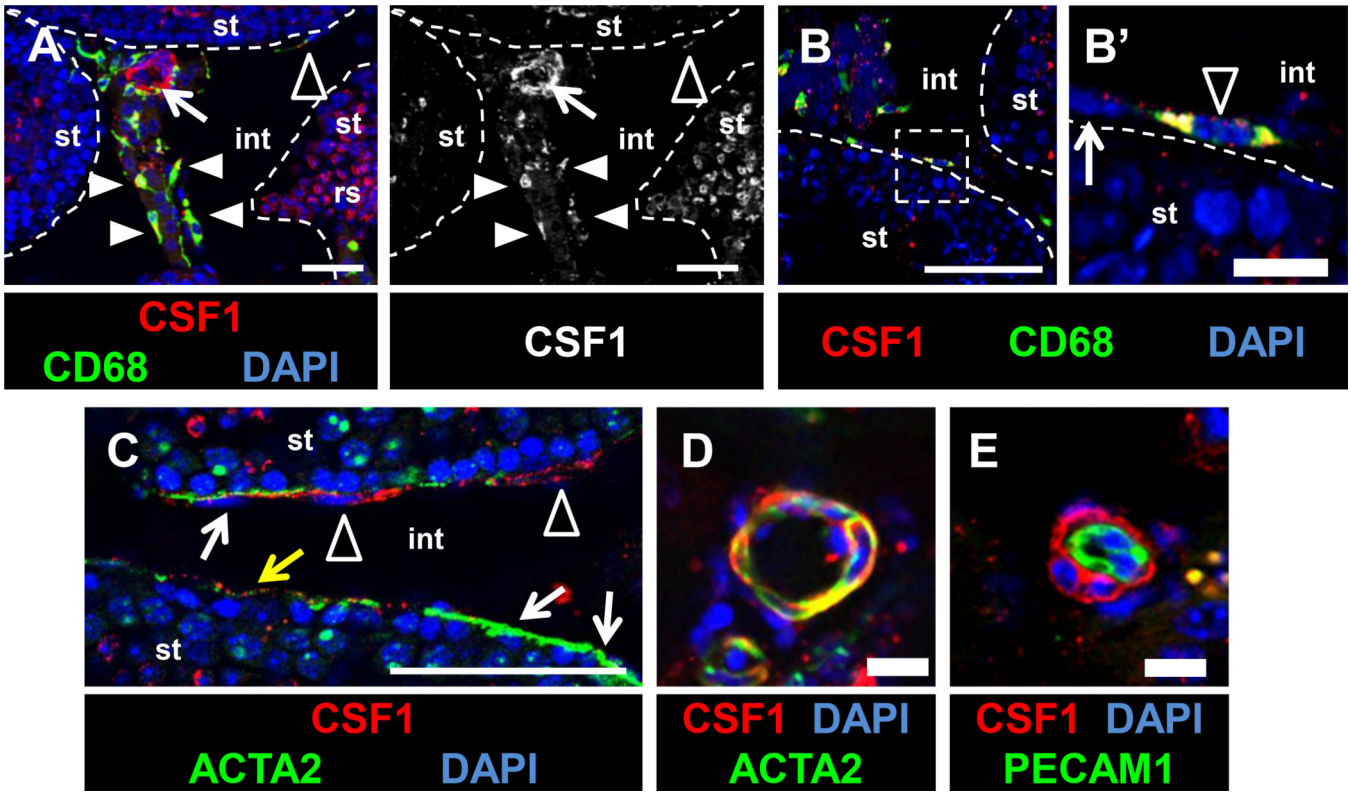

Figure 5. CSF1 protein is localized to macrophages and perivascular smooth muscle cells in the adult testis

CSF1 protein is detected within interstitial macrophages (A, white arrowheads), peritubular macrophages (A-C, black arrowheads), and vascular-associated cells (A, arrow), but is absent or weakly expressed in ACTA2-positive peritubular myoid cells (white arrows in B', C; yellow arrow in C points to myoid cell with weak CSF1 expression). CSF1 is detected in round spermatids ("rs" in A). Panel to the right of A is the CSF1-only channel from the image in A. Labeling perivascular smooth muscle cells with anti-ACTA2 antibody (D) or endothelial cells with anti-PECAM1 (E) reveals that vascular-associated CSF1 is specifically localized to perivascular smooth muscle cells. All images are from cryosectioned testes. Thin scale bar, 50 μm; thick scale bar, 10 μm.

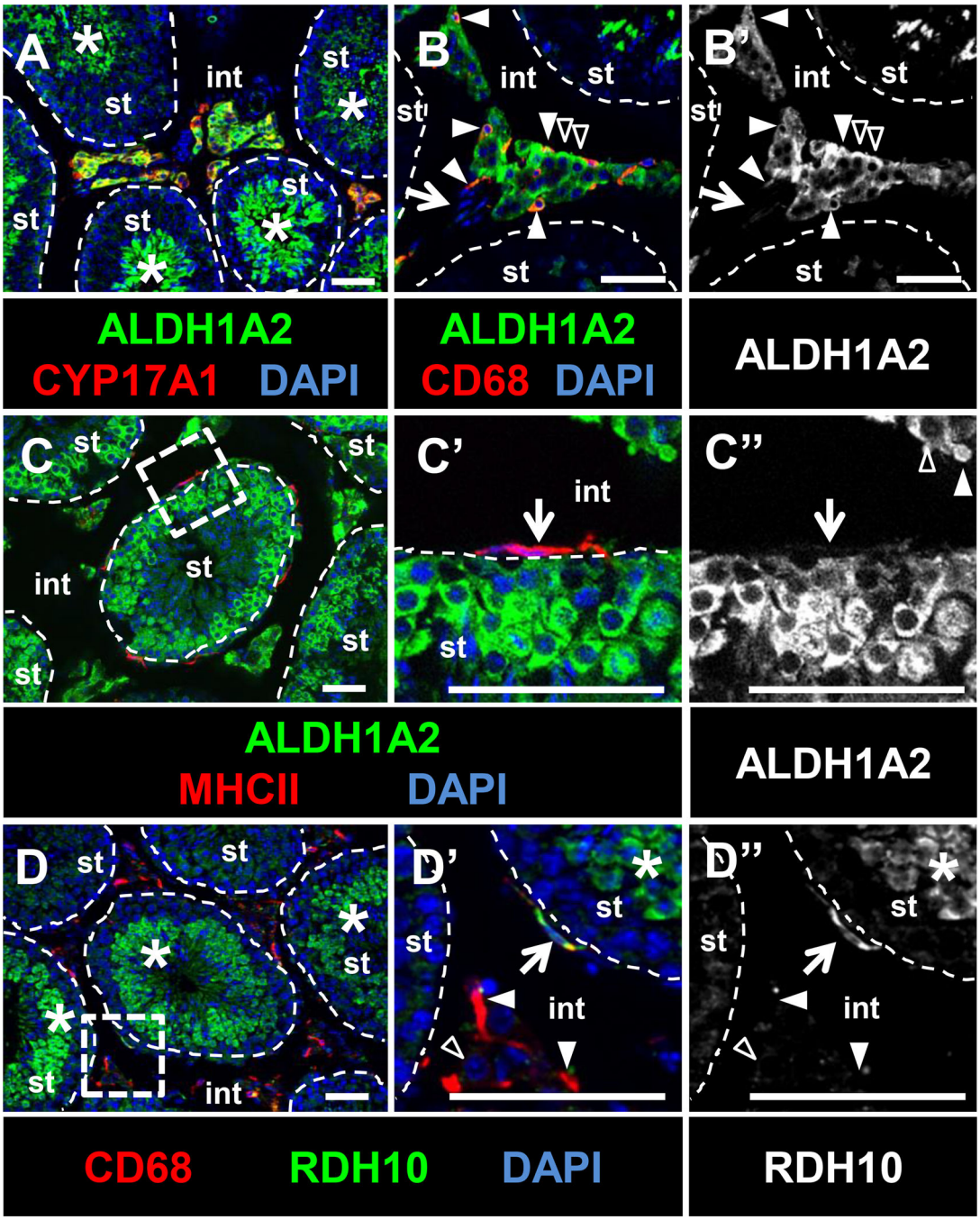

Figure 6. RA synthesis enzymes ALDH1A2 and RDH10 are expressed in testicular macrophages

(A–C) ALDH1A2 is detected within CYP17A1-positive Leydig cells (black arrowheads in B), interstitial macrophages (CD68-positive; B, white arrowheads), and germ cells (asterisks in A). ALDH1A2 is not expressed in vasculature (B, arrow), and is weakly expressed in MHCII-positive peritubular macrophages (C', arrow). RDH10 is detected in peritubular macrophages (D', arrow), but not in most interstitial macrophages (white arrowheads in D') or Leydig cells (black arrowhead in D'). RDH10 is detected in spermatids and other germ cells (D, D', asterisks). C' and D' are higher magnifications of the boxed regions in C and

D, respectively. B’ and C” are ALDH1A2-only channels for B and C’, respectively; D” is the RDH10-only channel for D’. All images are from cryosectioned testes. Scale bar, 50 μm.

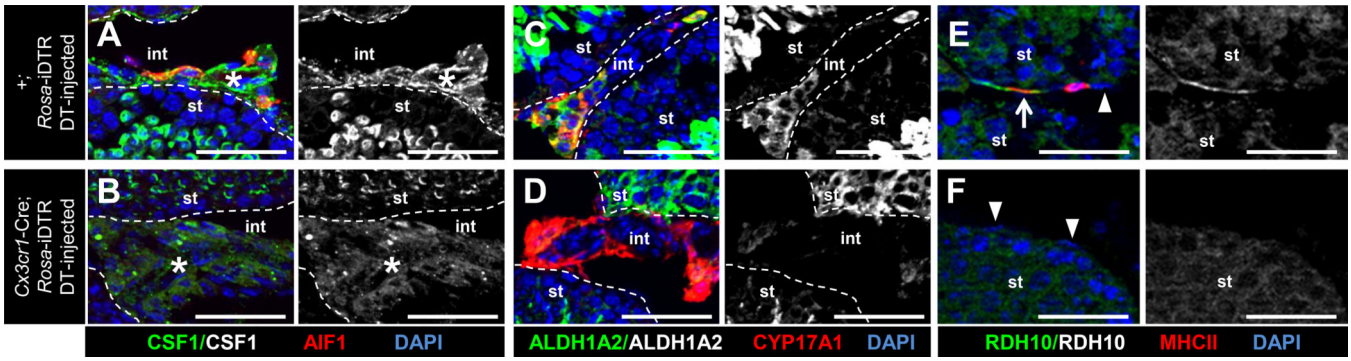

Figure 7. The expression of CSF1 and RA synthesis enzymes are dysregulated in macrophage-depleted adult testes

Immunofluorescent images of adult DT-injected Cre-negative *Rosa*-iDTR control (A, C, E) and DT-injected *Cx3cr1*-Cre; *Rosa*-iDTR macrophage-depleted (B, D, F) testes. Black-and-white images are CSF1-only (A, B), ALDH1A2-only (C, D), and RDH10-only (E, F) channels of the panel immediately to its left. In macrophage-depleted samples, CSF1 expression was no longer enriched in perivascular regions (A, B, asterisk), and ALDH1A2 (C, D) and RDH10 (E, F) expression were reduced. Arrow in E denotes a MHCII-positive, RDH10-expressing peritubular macrophage; arrowheads in E and F point to RDH10-negative peritubular myoid cells. All images are from cryosectioned testes. Scale bar, 50 μm.